JNCS
Journal of Nepal Chemical Society
March/April 2023, Vol. 43, No. 2, 110-124
ISSN: 2091-0304 (print)
DOI: https://doi.org/10.3126/jncs.v43i2.53356
RESEARCH ARTICLE

Preparation, Spectroscopic Analysis, and Biological Assessment of Heteroleptic Zr(II) and Pd(II) Complexes From Otc/Sal Mixed Ligands

Rohit Kumar Dev, Yuv RajSahu, Narendra Kumar Chaudhary, and Ajaya Bhattarai*

Department of Chemistry, Mahendra Morang Adarsh Multiple Campus, Tribhuvan University, Biratnagar, Nepal

*Corresponding author: **bkajaya@yahoo.com**

Submitted: 15 Oct 2022, 27 Dec 2022, accepted 07 Jan 2023

Abstract

The two new novel heteroleptic complexes of the type $[M(II)L_1.L_2]$ (M= Zr(II) & Pd(II), L_1= Oxytetracycline (Otc), and L_2 = Salicylaldehyde (Sal)) have been synthesized and analyzed by physical measurements such as CHN, pH,and conductivity. The conductivity data revealed the electrolytic nature of Pd(II)Otc/Sal and the non-electrolytic nature of the Zr(II)Otc/Sal metal complex of mixed ligand. The structural characterizations of the metal complex were approved by spectroscopic analysis methods, such as FT-IR, ^{1}H &^{13}C-NMR, UV/Visible, and ESI-MS studies. Thermal analysis (TGA/DTA) determines the thermal and kinetic stabilities of the metal complexes using a popular Coats-Redfern equation through which the activation parameters can be calculated easily. SEM can determine the surface morphology of metal complexes. The selected bond lengths, bond angles, final optimized energy, and geometry of complexes were obtained by running an optimization task in the 3D molecular modeling software program via Chem 3D Pro. 12.0.2. The final geometrical energy was found to be 921.7712 for Zr(II)Otc/Sal and 914.6006 Kcal/mol for Pd(II)Otc/Sal complexes. Based on the above study, Zr(II)Otc/Sal complex hastetrahedral geometry and the Pd(II)Otc/Sal complex has square planar geometry. The complexes were tested *in vitro* for antibacterial susceptibility study against various strains of clinical pathogenic bacteria such as *Staphylococcus aureus* (Gram-positive), *Proteus mirabilis,*and *Escherichia coli* (Gram-negative). For the antibacterial study, the Kirby-Bauer paper disc diffusion techniqueis applied by using 50, 25, and 12.5 µg/µL concentrations of the metal complex. All the synthesized complexes were found to have good antibacterial susceptibility against all tested pathogens.

Keywords: *Antibacterial activity, Heteroleptic complex, Mixed ligand, Oxytetracycline, TGA/DTA.*

Introduction

Diversity in the biochemical behavior of coordination compounds containing organic ligands with N, O, and S donor atoms has created a great impact on pharmacology because many such compounds are valuable in chemotherapeutics [1]. In the present day, the formation of a metal complex of mixed ligands between bioactive ligands (having binding sites) and 4d-transition metal (II) ions have gained much interest [2]. Coordination chemistry is an important property of metal ions that use different ligands [3]. Here, metal ions can show an inductive effect through the coordination site of the reaction and serve as oxidation-reduction via electron transfer reaction [4]. The transition metal complexes of the mixed ligand are mediators of bio-reaction and the technological process of the living organism [5]. In addition to biological functions, metal complexes are widely used in analytical, oxygen carriers, and organic catalysis reactions [6]. Currently, antibiotics

are one of the biggest global health threats to the modern scientific world. The factors associated with antibiotic resistance are compounded by overuse of antibiotics, abuse of treatment, and lack of financial support for complete treatment [7, 8, 9].

Oxytetracycline (Otc) is a broad-spectrum antibiotic of the tetracycline family used to prepare metal complexes. The Otc can inhibit protein synthesis for fixation on the 30s ribosomal subunit and can apply to both veterinary and human medical treatment. Because of hydroxyl and amino groups, Otc has both an acidic and basic nature [10, 11, 12]. Otc is mostly applied on farms and poultry farming. Because of its soluble nature, the animal's body cannot absorb the Otc compound [13]. Nearly 10% - 40% is only absorbed by animals and the rest 60% - 90% is excreted out into the environment, causing negative effects on the environment and human beings. Currently, anaerobic digestion (AD) is mostly used as a cost-effective and environmentally friendly process to check manure or sludge. Because of the high concentration in manure, the effects of antibiotics on AD can be easily investigated [14, 15].

The next compound, salicylaldehyde (Sal) along with its derivatives, can strongly coordinate with complexes and gives a variety of geometries [16]. Besides, their derivatives and diamines can behave as a potential catalysts for introducing oxygen into an organic compound [17]. Among the transition metal, zirconium acts as a homogenous catalyst because of its biological and pharmaceutical nature [18]. Similarly, palladium is a versatile metal that acts as a homogeneous and heterogeneous catalyst with a wide range of C-C coupling, hydrocarbon oxidation reactions, and C-H functionalization reactions [19, 20]. Palladium is a suitable metal for metallodrugs because of its structural properties that are like those with platinum and can exhibit *in vitro* cytotoxicity and their ions in coordination can form square planar geometries [21]. Today, many studies have proved that Otc is an old-generation antibiotic because of its resistance to many pathogenic bacteria [22, 23]. Because of the chelating and biological nature of the Zr(II) and Pd(II) complexes, it has been important to synthesize and characterize new derivatives of Otc.

In the current paper, we deal with the preparation of complexes by continuous heating and refluxing the equimolar mixture of the primary ligand (Otc), secondary ligand (sal), and 4d-transition metal salts [M=Zr(II) and Pd(II)]. This investigation was further extended to physicochemical and spectroscopic characterization: FT-IR, ^{1}H &^{13}C-NMR, UV/Visible, ESI-MS, TGA/DTA, and SEM. The metal complexes were also done through molecular modeling and antibacterial susceptibility against various strains of bacteria.

Experimental Methods

Materials and reagents

The reagents and chemicals employed for the synthesis of metal complexes were of AR grade and were used without further purification. The used chemicals such as oxytetracycline hydrochloride (TCl), MHA, $PdCl_2$ (Himedia), $ZrOCl_2.8H_2O$, and salicylaldehyde (Loba Chemie Pvt. Ltd) were collected from a supplier. Distilled ethanol and triple–distilled water were used during the synthesis process. High-grade borosilicate glassware was used during the research.

Physical measurements

The percentage of CHN was done by a micro analyzer, Euro-E 3000 for CHN analysis. pH was measured at 25 $°C$ ± 0.1 $°C$ on Eutech Instrument, 2700 pH/Mv/°C/°F meter. The conductivity was measured by a digital conductivity meter called auto-ranging/TDSmeter TCM 15+ instrument. The instrument called VEEGO ASD-10013 programmable measures the melting point of the metal complex. In the range of 4000-400 cm^{-1}, the FT-IR spectrum was recorded by Perkin Elmer Spectrum II instrument under KBr pellets.The ^{1}H and ^{13}C-NMR spectra wererecordedon a Bruker AvII (400 MHz) instrument using DMSO-d6 solvent at room temperature. Electronic absorption spectra were plotted in the range of 260-280 nm on a Varian Cary 5000 instrument in DMSO at 0.001M concentration. The ESI-MS spectra were recorded using an instrument called a water UPLC-TQD mass

spectrometer. At a room temperature of 756 °*C*, the kinetic and thermal stabilities of the complexes were calculated from Perkin Elmer Diamond TGA/ DTA instrument with a linear heating rate of 10°*C* under a nitrogen atmosphere. The SEM instrument (JEOLJSM-6390 LV) helps to detect the surface morphology. Molecular modeling was done through the 3D modeling software program, Chem 3D Pro 12.0.2. Antibacterial activities were performed at the microbiological laboratory, Department of Microbiology, M. M. A.M. Campus, T.U., Biratnagar, Nepal.

Synthesis of the metal complex of mixed ligands

The Zr(II)Otc/Sal and Pd(II)Otc/Sal metal complexes were prepared simply as mentioned below. To 10 ml of aq. Solution of $ZrOCl_2$/ 10% HCl ethanolic solution and $PdCl_2$ (0.3565g, 2 mmol) was mixed with continuous stirring and heating 70% ethanolic solution (20ml) of Otc (0.9945g, 2mmol). To this following mixture, salicylaldehyde (0.2 ml, 2 mmol) was mixed in a drop-wise manner and stirred for an hour. The stirred solution was then refluxed for 8 h and ammonia solution was added to make a pH of 7, resulting in precipitates. The precipitate was filtered and then washed with ethanol.Thus, the obtained

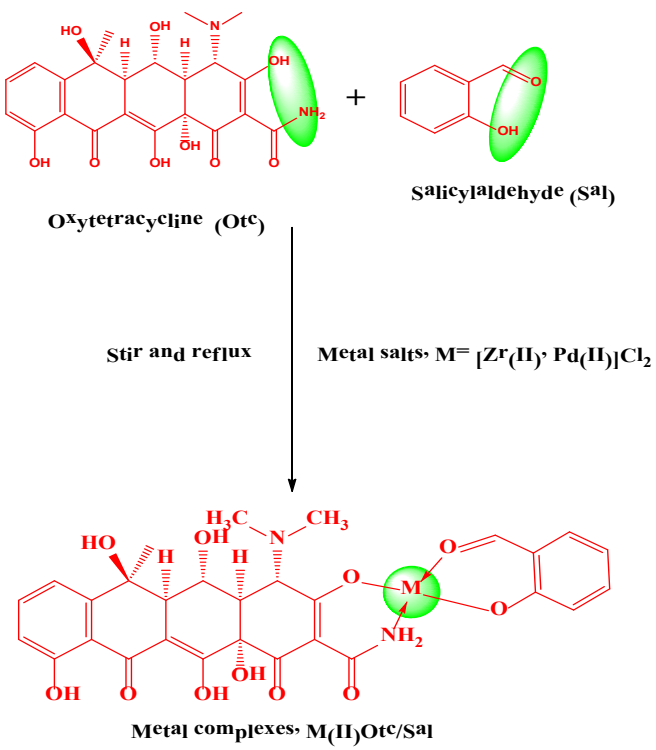

Scheme 1: *Synthetic route for the preparation of the metal complex.*

dried precipitate was recrystallized and kept inside a vacuum desiccator over anhyd. $CaCl_2$. Finally, the dried complexes were stored in a vial for further use [24, 25]. The percentage yield was 50-60%. The synthetic route for M-Otc/Sal [M=Zr(II), Pd(II)] complexes are reported in **Scheme 1**.

Antibacterialsusceptibility test

Zr(II)Otc/Sal and Pd(II)Otc/Sal complexes were screened for their anti bacterial susceptibility test with the help of human pathogenic bacteria such as *Staphylococcus aureus* (Gram-positive), *Escherichia coli,* and *Proteus mirabilis* (Gram-negative). The Kirby-Bauer paper disc diffusion method is applied for the study. For the test, 30% DMSO solvent of various concentrations such as 50, 25, and 12.5 µg/µL was selected for the test solution. The blank disc (5mm diameter) was prepared from filter paper (Whatman No. 1) using a punching machine. In a freshly prepared nutrient agar medium, the bacterial culture was revived and kept for a few hours in an incubator at 37 °*C* for the complete growth of the organism. MHA media, blank paper discs, and Petri plates were prepared and sterilized inside the autoclave. Under UV laminar flow, the media was solidified to prevent the contamination of bacteria. The solidified MHA plates were seeded with freshly revived bacteria and sterilized blank paper discs. 10 µL of test solutions (complex) was loaded into the disc under UV laminar flow. To compare the effectiveness of a metal complex, amikacin behaves as positive control while a blank disc soaked in DMSO as solvent control. While doing the above activities, the used plates are placed inside the incubatorat 37 °*C* for 24 h. Finally, the antibiogram zone measuring scale measures the diameter of the inhibition zone (in mm) [26, 27].

RESULTS AND DISCUSSION

Properties of the complexes

The complexes explained in this current article were characterized by physicochemical and spectroscopic methods. The satisfactory result obtained from micro elemental analysis exhibited that the complexes are of a 1:1 molar ratio. Here, all the synthesized complexes are thermally stable and are not affected by air and

Table 1: *Physical and microanalytical measurement data of Zr(II)Otc/Sal and Pd(II)Otc/Sal complexes*

Complexes	Empirical formula	Mol. Weight	Color	m.p.	Calculated (found)%				
					C	H	N	O	M
Zr(II)Otc/Sal	$C_{29}H_{28}ZrN_2O_{11}$	671.76	Black	>260	51.85	4.20	4.17	26.20	13.58
					(51.80)	(4.26)	(4.15)	(26.24)	(13.55)
Pd(II)Otc/Sal	$C_{29}H_{28}PdN_2O_{11}$	686.96	Black	>260	50.70	4.11	4.08	25.62	15.49
					(50.67)	(4.08)	(4.17)	(25.84)	(15.24)

Table 2: *The infrared spectral absorption data of Zr(II)Otc/Sal and Pd(II)Otc/Sal metal complex in cm^{-1}*

Complexes	υ(O-H/NH)	υ(CH) Methyl	υ(C=O)	υ(C=C) Aromatic	υ(C-N)	υ(C-O)	υ(M-O)
Zr(II)Otc/Sal	3426	3055	1614	1502	1456	1240	552
Pd(II)Otc/Sal	3428	2941	1622	1455	1387	1230	603

moisture. The change in color during complex formation is because of the metallation of metal ions with ligands and different electronic transitions like π bonding or non-bonding or by the free electron. In the presence of auxochrome, the chromophore exhibits electronic absorption of the spectrum in the UV/ Visible region and finally gives color to the complexes. The solubility behavior of metal complexes was investigated using various solvents such as water, ethanol, methanol, acetone, chloroform, DMF, and DMSO. All the complexes are miscible in DMF and DMSO solvents while immiscible in water.

The higher value of conductivity shows a complexation behavior of metal ions. The obtained data showed that the synthesized metal complexes have electrolytic nature. The complex nature of the ligand during the formation of the metal complex is because of the deprotonation and change in pH. The physical and microanalytical measurement data Zr(II) Otc/Sal and Pd(II)Otc/Sal complexes were reported in Table 1.

Spectroscopic parameters

3.2.1 FT-IR spectroscopic study

Figure 1 and S1, show the FT-IR spectrum of the Zr(II)Otc/Sal and Pd(II)Otc/Sal complexes, and their characteristic absorption data were presented in Table 2. The intense peaks at 3426 cm^{-1} and 3428 cm^{-1}, are assigned to υ(OH/NH) stretching vibration [28, 29]. The C-H stretching and bending vibration lies in the region of 3061 cm^{-1} and 2941 cm^{-1} respectively [30, 31]. Similarly, the strong absorption bands with stretching vibration of the carbonyl (C=O) groupwere seen at 1614 cm^{-1} and 1622 cm^{-1} regions in the spectrum [32, 33]. The aromatic υ(C=C) absorption bands are at 1502 cm^{-1} and 1455 cm^{-1} respectively [34]. The complexes at (1456 and 1387) $cm^{-1}$are due to a characteristic band υ(C-N); this band denotes the carbon-nitrogen bond order intermediate between a single bond. Thus, metal shows the coordination of nitrogen with ions [35]. Similarly, the peak at 1240 cm^{-1} and 1230 cm^{-1} are due to υ(C-O) [36, 37]. In addition, the peaks at 552 cm^{-1} and 603 cm^{-1}, were assigned to the υ(M-O) respectively, which is proved by the presence of the IR band of the low-frequency band of the coordination mode [38, 39].

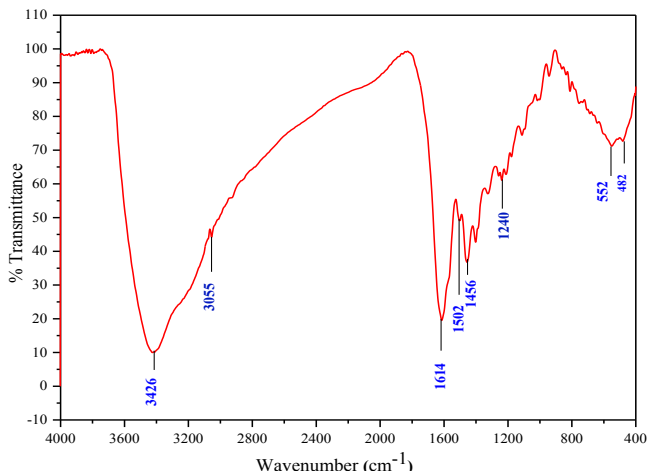

Figure 1. *The infrared spectrum of the Zr(II)Otc/Sal metal complex*

^{1}Hand^{13}C-NMR spectroscopic study

The ^{1}H-NMR gives information about the chemical shift value and proton environment of the complexes. The chemical shift data are reported in Table S1 and Figure S2 and S3. In the Zr(II)Otc/Sal metal complex, aromatic ring protons are assigned as multiplet between δ7.023-7.279 ppm. These protons moved upfield slightly to confirm the coordination of metal ions with the ligands [40]. A single peak at δ1.047-1.082 ppm, was assigned to the methyl proton. A high-intensity peak at δ2.543 ppm is observed and is supposed to be of DMSO solvent and the peak at δ3.399-3.406 ppm is assigned to be of $–NCH_3$. In the same way, in the Pd(II)Otc/Sal metal complex, aromatic ring protons are observed and are assigned as multiplet between δ6.632-7.516 ppm [41]. These protons moved upfield slightly to confirm the coordination of metal ions with the ligands. A single peak at δ1.040-1.075 ppm, is assigned to a methyl proton. A high-intensity peak observed at δ2.500 ppm is supposed to be of DMSO solvent and the peak at δ3.412-3.465 ppm is assigned to be of the $–NCH_3$ group [42]. Hence, all the values in the peak of the ^{1}H-NMR spectra showed a good relationship with the proposed structure of the complexes.

The ^{13}C-NMR spectral study gives knowledge regarding the different carbon atoms, mode of bonding, and geometry of the complexes. The spectra were recorded in the DMSO-d_6 solvent and their pictorial representation was reported in Figure S4 and S5 and Table S2. In the ^{13}C-NMR spectra of the Zr(II)Otc/Sal metal complex, the carbon resonance signals of methyl, DMSO, and CH group appeared at δ(18.366, 40, and 55.821-55.942) ppm respectively [43]. Similarly, in the Pd(II)Otc/Sal metal complex spectra, the signal observed at δ137.147 ppm in the spectrum was assigned to the aromatic carbon signal, which remains the same in the literature. The upfield shift of the carbon signal, which appears at δ34.257 ppm confirms the $–CH_2$ group. The signals that appeared at δ(40,71.543, and 84.502) ppm in the spectra were assigned to be DMSO, -CH, and C=C groups respectively [44]. Thus, the (^{1}H and^{13}C)-NMR spectra, confirm all measured values of carbon atoms to their chemical shift value.

Mass spectroscopicstudies

ESI-MS spectrum helps to explain the molecular weight and structure of ligand and metal complexes. The spectrum also displays the fragmentation pattern and the most fragile points in the compound. The ESI-mass spectrum of the metal complexes recorded important peaks and their intensities for molecular ions, as shown in Figure 2 and S6. Besides the most abundant peaks, there are many fewer abundant peaks seen in the spectrum that depends on the ligand. The mass spectrum of metal complexes showed a well-defined peak at m/z-671 and 687 amu signifies molecular-ion peak $[M+H]^{+}$. assigned to the molecular formula of Zr(II)-Otc/Sal and Pd(II)-Otc/Sal metal complexes ($C_{29}H_{28}ZrN_2O_{11}$ and $C_{29}H_{28}PdN_2O_{11}$), which confirms that the stoichiometry ratio of the metal-to-ligand ratio is 1:1. The base peak lies at m/z-176 and m/z-365 amu respectively in Zr(II)-Otc/Sal and Pd(II)-Otc/Sal metal complexes. There is also another additional peak called fragment ion peak lies near m/z 665, 614, 608, 566, 538, 536, 502, 461, and 453 amu in the Zr(II)-Otc/Sal complex, while at m/z 659, 620, 600, 563, 510, 443, 426, and 410 amu respectively, for the Pd(II)-Otc/Sal metal complex [45, 46].

Electronic absorption spectra

The UV/Visible spectroscopy measures the geometry of the metal complex and the spectra determine the effect of splitting of d-orbital during complexation. At room temperature, the significant electronic spectral data of Zr(II)Otc/Sal and Pd(II)Otc/Sal complexes were measured in DMSO solvent from 200 to 630 nm using the same solvent as the blank. The spectral data and absorption bands were reported in Figure S7 and Table S3. The Zr(II)Otc/Sal metal complex showed the spectral bands at 379 nm, which corresponds to the ligand to metal-charge-transfer (Zr→L) or π→π* transition [47, 48]. The Zr(II) metal complex has no d-d transition because of its d^0 electronic configuration, and therefore, the complex has tetrahedral geometry and diamagnetic nature [49]. Similarly, the electronic spectrum of Pd(II) complexes showed four bands at 265, 271, 386, and 457 nm respectively. These are attributed due to the intraligand π→π as well as spin-allowed LMCT

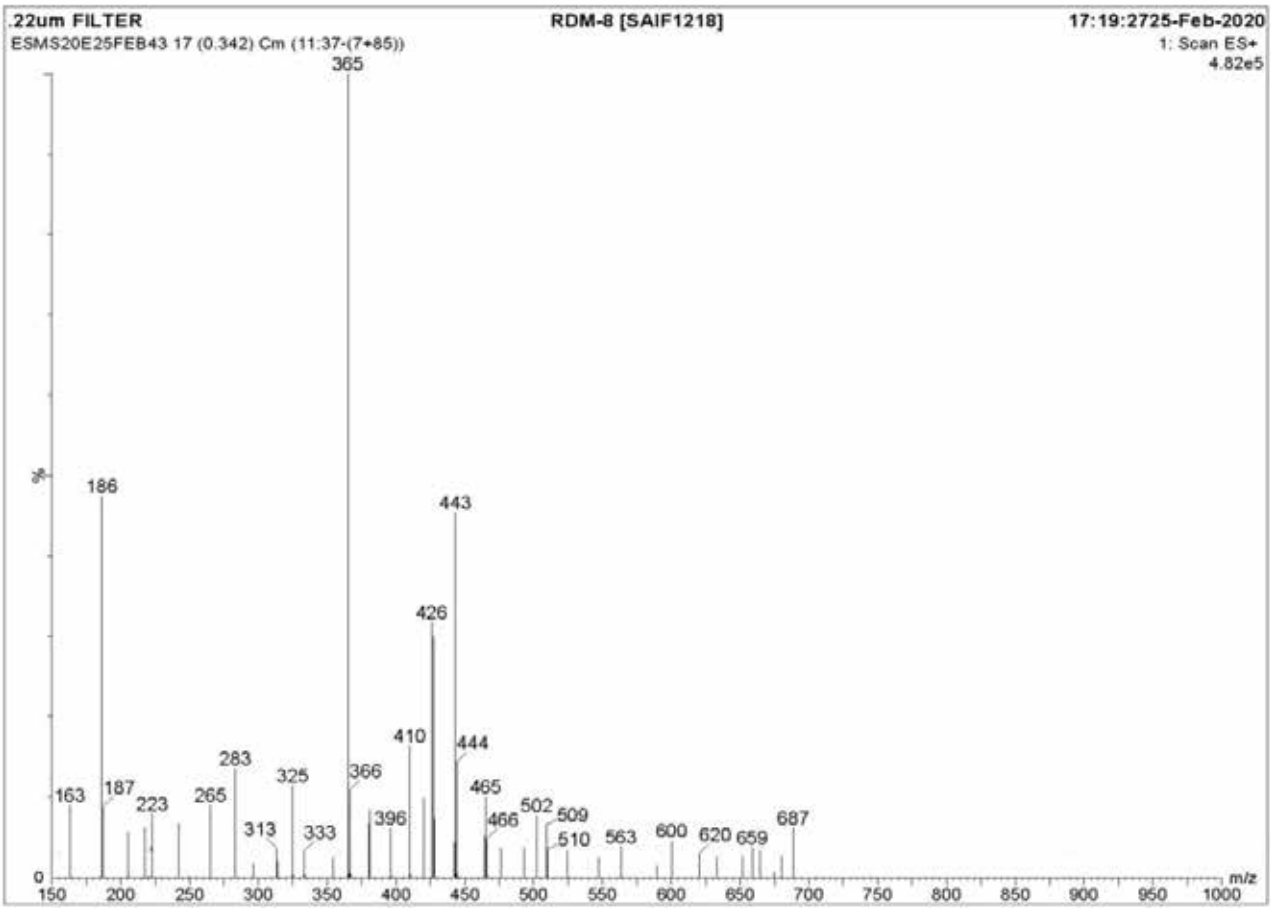

Figure 2. *Mass spectrum of the Pd(II)Otc/Sal metal complex*

d-d transition. The complex at 386 nm is attributed to the 1A2g→1B1g. The above transitions showed that the complex has a diamagnetic nature, and this assignment refers that the complex has square planar coordination around the metal ions [50, 51, 52, 53].

TGA/DTAanalysis

Thermal gravimetric analysis techniques help to determine the thermal behavior of the complexes. This technique also deals with decomposition steps, temperature range, % weight loss, and decomposition products. At room temperature (40.15°*C*- 755.5°*C*), the analysis was performed with a linear heating rate of 10°*C*/min under a nitrogen atmosphere. The data of thermal decomposition was calculated and is presented in Table S4, which shows a better result than the data for the microanalytical. Consistent results were drawn from the current research work. In the thermogram of the Zr(II)Otc/Sal complex, the decomposition occurs at three different phases with a temperature range of 62.42°*C* - 750.58°*C*. The first decomposition step occurred at 62.42°*C* - 132.18°*C,* with a mass loss of 1.19% (-0.433 mg), which denotes the removal of hydrated water molecules. The second step appeared at 187.96°*C* - 291.00°*C,* with a mass loss of 1.51 % (-0.350 mg). The final phase decomposition at 490.46°*C* -750.58°*C*, representing a total mass loss of 7.56 % (-0.929 mg) from the metal complex resulting in a stable residue as metal oxide (ZrO+C). Similarly, the thermogram of the Pd(II) Otc/Sal complex showed that the decomposition occurs in two different phases between a temperature range of 45.34°*C*–252.87°*C*. The first decomposition step occurred at 45.34°*C*–69.61°*C,* with a mass loss of 4.31% (-2.535 mg), which denotes the removal of hydrated water molecules. The second step appeared at 218.62°*C*–252.87°*C,* with a mass loss of 8.69% (-2.751 mg) in the ligand from the metal complex, leaving behind a stable residue as metal oxide (PdO+C). The metal complexes showed their thermograms as presented in Figure 3 and S8.

Table 3. *Thermodynamic and kinetic parameters of the Zr(II)Otc/Sal and Pd(II)Otc/Sal complexes*

Complexes	r	A(s^{-1})	Tmax(K)	E*(kj/mol)	ΔS*(j/kmol)	ΔH*(kj/mol)	ΔG*(kj/mol)
Zr(II)Otc/Sal	-0.99501	1727.835	365.86	1273.871	-184.630	-1766.642	65754.543
	-0.99424	890.887	513.75	968.248	-192.964	-3303.069	95831.9546
	-0.98972	386.589	868.33	641.508	-204.268	-6577.787	170794.268
Pd(II)Otc/Sal	-0.99622	2.99740	324.508	0.63236	-236.49	-2697.33	-74045.57
	-0.99043	0.77258	504.75	0.305955	-251.43	-4196.19	122714.24

Kinetic parameter study

The thermodynamic and kinetic parameters of metal complexes having different decomposition phases were calculated by using a very well-known equation called the Coats-Redfern equation. The parameters were graphically plotted with the help of the Coats-Redfern equation (1).

$$\ln\left[-\frac{\ln(1-\alpha)}{T^2}\right] = \ln\left[\frac{AR}{\beta E^*}\right] - \frac{E^*}{RT} \quad (1)$$

Here, T denotes the temperature of the DTG curve, β and R represent the linear heating rate, and the Universal gas constant. A and E^* represent the Arrhenius pre-exponential factor and energy of activation. By applying a straight line equation, $y = mx + c$, a linear plot on the left-hand side vs $1/T$, gives a slope $(-E^*/R)$ that determines the energy of activation. Finally, ΔS^*, ΔH^*, and ΔG^* can be calculated by applying the successive relations 2-4.

$$\Delta S^* = R \ln\left[\frac{Ah}{K_B T}\right] \quad (2)$$

$$\Delta H^* = E^* - RT \quad (3)$$

$$\Delta G^* = \Delta H^* - T\,\Delta S^* \quad (4)$$

Here, kinetic and thermodynamic parameters of the different decomposition phases [54, 55, 56] are calculated and reported in Tables 3 and S4. The following remarks can be derived from the above results:

1. On moving to another decomposition step, the activation energy (E^*) value decreases. Hence, the rate becomes weak and shows higher stability of metal complexes.
2. In most of the decomposition steps, the entropy of activation having a negative value ($-\Delta S^*$) signifies the slowdown of the reaction condition having more ordered activated complexes and reflects spontaneous decomposition steps.
3. The negative value of enthalpy ($-\Delta H^*$) signifies the exothermic process of decomposition.
4. The positive value of Gibb's free energy of activation ($-\Delta G^*$) reflects its non-spontaneous nature.

Thus, the calculated data of the correlation coefficient (r) obtained with the help of the graphical plot signifies a better fit with the linear function.

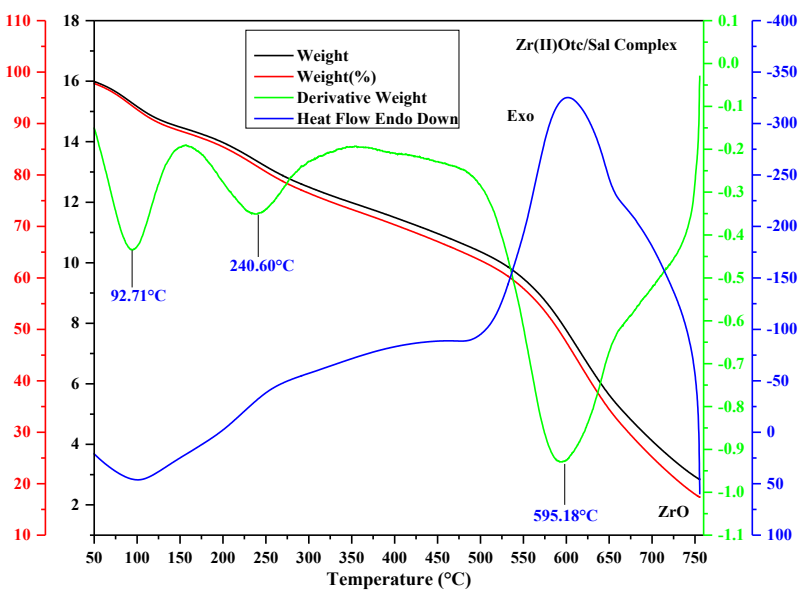

Figure 3. *Thermogram of Zr(II)Otc/Sal metal complex*

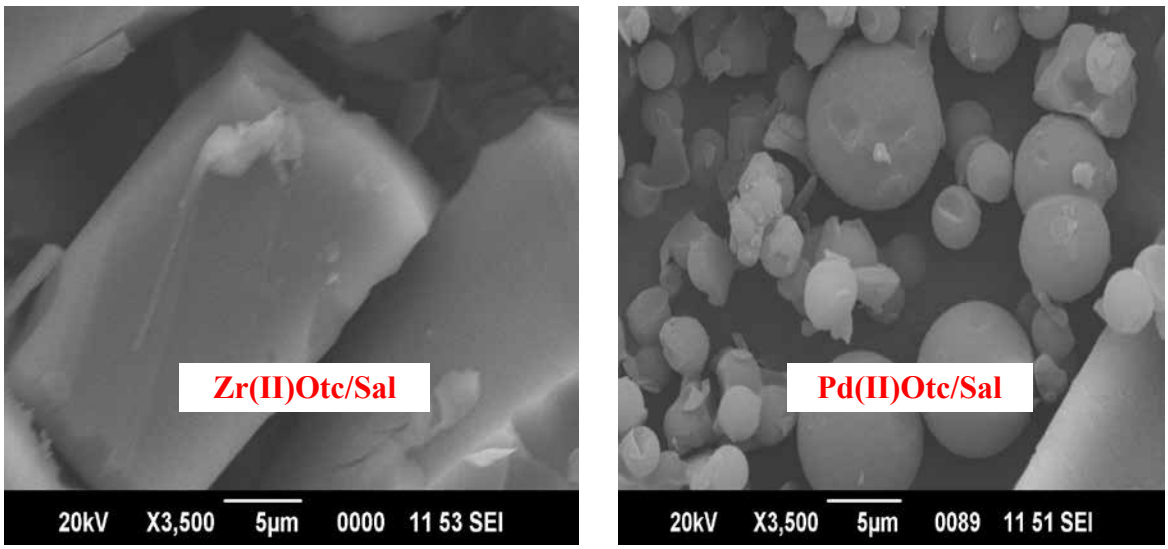

(a) (b)

Figure 4. *SEM micrograph of Zr(II)Otc/Sal and Pd(II)Otc/Sal metal complexes*

SEM study of M(II)-Otc/Sal metal complexes

SEM (scanning electron microscopy) is an instrumental method that gives knowledge regarding the surface morphology comparison of metal complexes. The unique characteristics of the micrograph will indicate the shape, size, arrangement, ductility, and strength of the metal complexes. The micrograph of Zr(II)Otc/Sal complex (a) displays the surface particles are clear, smooth, and not aggregated, but besides the metal ion, the surface particles become rough and fully covered [57]. Similarly, Pd(II)Otc/Sal metal complex (b) revealed that the complex exhibits uniform and spherical morphology on its surface [58], and is presented in Figure 4.

Molecular Modeling

Molecular modeling investigates the clear and deep geometry of the proposed structure of the complex. Here, the modeling was performed througha 3D modeling software called the Chem 3D Pro12.0.2 program. After geometrical optimization, the complexes Zr(II)Otc/Sal and Pd(II)Otc/Sal have tetrahedral and square planar geometries with final geometrical energies of 921.7712 and914.6006 (kcal/mol), resulting in stable stability. The optimized structures are shown in Fig.-S9 and S10. With the help of the MM2 program, energy minimization was repeated many times to note the minimum energy value. The difference in the values of M-N and M-O in the complexes further shows the metallation of ligands with the metal ions [59]. The computational findings showed that the proposed structure and geometry of complexes are in better agreement with the literature. Table S5 represents the data of selected bond length, bond angle, final optimized energy, and geometry of the metal complexes.

Swiss ADME study

The web tool server (Swiss ADME) is used to calculate the parameters such as absorption, distribution, metabolism, and excretion as well as physicochemical properties [60, 61]. By this computation, the lipophilicity, pharmacokinetics, drug-likeness, and medicinal chemistry of the compound are depicted in Figure S12 and S13 [62]. Here, the drug-likeness is estimated as whether the molecule is considered an oral drug according to its availability. Pharmacokinetics properties such as BOB (Blood-brain barrier), GIA (gastrointestinal absorption), and penetration through P-gp substrate were studied and compared with oxytetracycline and salicylaldehyde as a controlled drug. When compared to the allowed value for polarity TPSA (Total polar surface area -217.15 Å), lipophilicity (log $P_o/W < 1$), solubility (log $S < 1$), size (MW- 671.76 g/mol), log K_p(skin permeation-10.27 Cm/S). These all values are reported in Table 6. The above metal complexes showed calculated values within these limits. Finally,

Table 4. *The data of antibacterial growth inhibition zone of Zr(II)Otc/Sal and Pd(II)Otc/Sal metal complexes*

Complexes	The diameter of the zone of inhibition in (mm)								
Pathogenic Bacteria	*S. aureus*			*P. mirabilis*			*E. coli*		
Concentrations (μg/μL)	50	25	12.5	50	25	12.5	50	25	12.5
Zr(II)Otc/Sal complex	23	21	20	14	12	10	12	11	10
Pd(II)Otc/Sal complex	18	17	12	18	13	12	10	9	8
Amk (30mcg/disc)	21			21			14		
OTC-Ethanol	37			33			28		
OTC-DMSO	41			34			29		
DMSO	0			0			0		

the complexes showed a low GIA (gastrointestinal absorption potential) and ability to cross the BBB (blood-brain barrier). These results eventually led to the conclusion that the prepared complexes may be a better candidate as an antibacterial drug soon [63]. The predicted description showed that the complexes have good lipophilicity and human intestinal absorption. In addition, it is easy to pass through the BBB, inhibiting various CYP metabolic enzymes to act as β-glycoprotein substrates, and ultimately has drug-like properties as adopted by such as Lipinski, Ghose, Egan, and Muegge. This rule does not violate the test [64].

Antibacterial Susceptibility Study

The *in vitro* antibacterial susceptibility activities of Zr(II)Otc/Sal and Pd(II)Otc/Sal metal complexes were done by measuring the zone of inhibition via the Kirby-Bauer paper disc diffusion technique [65, 66]. For the antibacterial test, two strains of bacteria were selected: *Staphylococcus aureus (gram-positive*), *Escherichia coli,* and *Proteus mirabilis (gram-negative*). In DMSO solvent, the three different concentrations (50, 25, 12.5 μg/μL) were prepared from the metal complex. These concentrations were selected for their antimicrobial activity. The data for the growth inhibitionz one is presented in Table 4 along with bar graphs as shown in Figures 5, 6, 7, and S11. To differentiate the efficiency of the targeted complex, amikacin (30 mcg/disc) acts as the positive control while the blank disc soaked in DMSO is the negative control. The observation of all the complexes showed better results at higher concentrations and considerable activity at a lower concentrations. Hence, the *in vitro* antibacterial activity showed that the complexes are bacteriostatic. The intensity of the antibacterial action of ligands and complexes depends upon the type of species of microorganisms. The tested complexes significantly showed lower antibacterial activity compared to commercial antibiotics [67, 68]. From the Table, Zr(II)Otc/Sal complex shows more reactive than Pd(II)Otc/Sal complex. Thus, the above complexes show better activity against the tested strains of bacteria.

The effect of metal ions on the surface of the cell membrane of an organism determines the high activity of the complex. Here, metal chelates contain both polar and non-polar groups that help for easy permeation into the cell and tissues of microorganisms, causing the decrease of the biochemical potential of the cell [69]. These antibacterial findings in our research work will be new hope for the development of more efficient metal-based therapeutic drugs in the future.

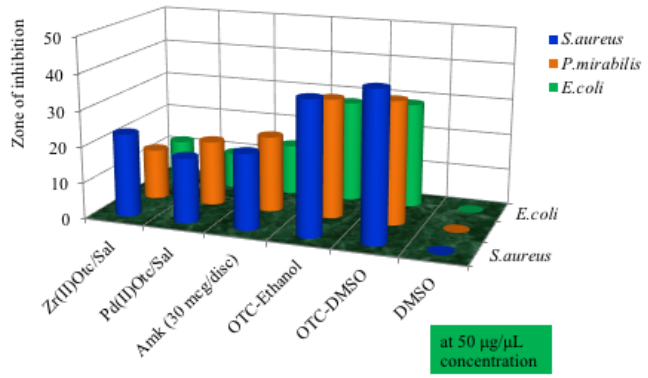

Figure 5. *Bar graph for the antibacterial activity study of metal complexes at 50 µg/µL concentration.*

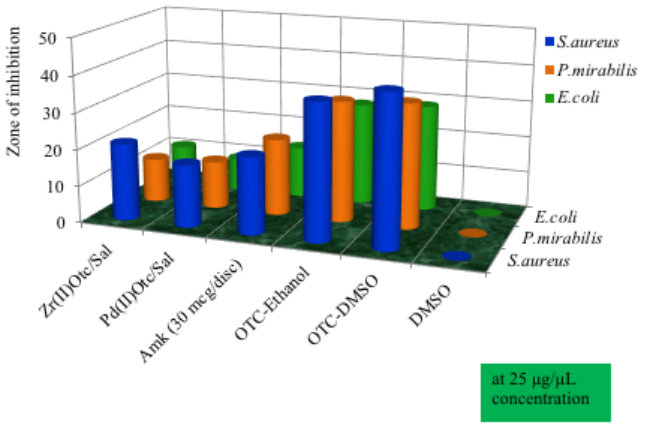

Figure 6. *Bar graph for the antibacterial activity study of metal complexes at 25 µg/µL concentration.*

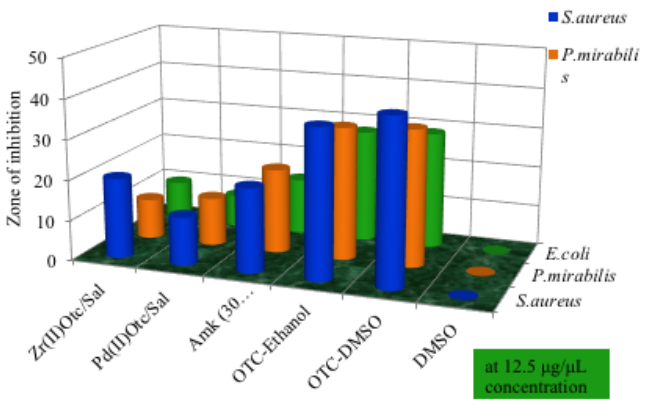

Figure 7. *Bar graph for the antibacterial activity study of metal complexes at 12.5 µg/µL concentration.*

CONCLUSION

The current article deals with the successful synthesis of two novel metal complexes (Zr(II)Otc/Sal and Pd(II) Otc/Sal) of the mixed lig and with the complexation of oxytetracycline, salicylaldehyde along with the metal ions. The formation of the synthesized complexes was monitored by physical and spectral methods. Metal complexes are colored, amorphous, soluble in organic solvents (DMSO and DMF), and insoluble in water. The FT-IR, UV/Vis., and NMR spectral data reveal the complexation of metal ions with amide N atom of C2 and O at C3 of oxytetracycline in ring A and O atom of salicylaldehyde. Electronic absorption data showed tetrahedral and square planar geometries for the Zr(II)Otc/Sal and Pd(II)Otc/Sal metal complexes. The selected bond lengths, bond angles, and optimized bond energies obtain from the 3D modeling software also suggest the above geometry. From the Coats-Redfern equation, the activation energy decreases on moving to another decomposition step, so the rate becomes weaker and the metal complexes show higher stability. The negative value of the activation energy indicates the slowness of the reaction condition and indicates the spontaneous decomposition steps. SEM images characterize the surface morphology of the metal complexes. The antibacterial evaluation showed significant antibiotic action against human clinical pathogens. The prepared complexes also showed antibacterial activity. Here, Zr(II)Otc/Sal metal complex revealed a better antibiotic effect than Pd(II)Otc/Sal. Therefore, these research works have created a golden opportunity for researchers and chemists to develop a more potent drug in the field of pharmaceutical science and also for the welfare of mankind.

Conflicts of Interest

There is no conflict of interest reported by the author.

Acknowledgments

One of the authors (Rohit Kumar Dev) is highly grateful to the NAST (Nepal Academy of Science and Technology), Khumaltar, Lalitpur, Nepal for funding the research work. The authors are also grateful to STIC Cochin, CSIR-CDRI, Lucknow, NBU Siliguri, and SAIF IIT Bombay, India for providing spectroscopic characterization facilities.

References

1. K. Sharma, R. V. Singh, and N. Fahmi, Palladium(II) and platinum(II) derivatives of benzothiazoline ligands: Synthesis, characterization, antimicrobial and antispermatogenic activity, Spectrochimica Acta - Part A: Molecular and Biomolecular Spectroscopy, 2011, 78(1), 80-87. (DOI: 10.1016/j.saa.2010.08.076)
2. S. Shobana, P. Subramaniam, L. Mitu, J. Dharmaraja, and S. A. Narayan, Synthesis, structural elucidation, biological, antioxidant and nuclease activities of some 5-Fluorouracil–amino acid mixed ligand complexes, Spectrochimica Acta - Part A: Molecular and Biomolecular Spectroscopy, 2015, 134, 333-344. (DOI: 10.1016/j.saa.2014.06.093)
3. A. Abebe, and T. Hailemariam, Synthesis and Assessment of Antibacterial Activities of Ruthenium(III) Mixed Ligand Complexes Containing 1,10-Phenanthroline and Guanide, Bioinorganic Chemistry and Applications, 2016, 1-9. (DOI:10.1155/2016/3607924)
4. H. Khan, N. Daraz, M. N. Khan, M. Said, N. Akhtar, A. Badshah, A. S. Khan, and M. Ali, Synthesis, Structural Characterization, and Evaluation of the Biological Properties of Heteroleptic Palladium(II) Complexes, Bioinorganic Chemistry and Applications, 2014, 1-7. (DOI: 10.1155/2014/916361)
5. A. K. Molodkin, N. Y. Esina, M. V. Tachaev, M. N. Kurasova, Mixed-Ligand Palladium(II) Complexes with Amino Acids, Cytosine, and Adenine, Russian Journal of Inorganic Chemistry, 2007, 52(10), 1567-1669. (DOI: 10.1134/S0036023607100166)
6. H. F. A. El-Halim, G. G. Mohamed, and E. A. M. Khalil, Synthesis, spectral, thermal and biological studies of mixed ligand complexes with newly prepared Schiff base and 1,10-phenanthroline ligands, Journal of Molecular Structure, 2017. (DOI: 10.1016/j.molstruc.2017.05.092)
7. A. J. Alanis, Resistance to Antibiotics: Are We in the Post-Antibiotic Era?, Archives of Medical Research, 2005, 36, 697-705. (DOI: 10.1016/j.arcmed.2005.06.009)
8. A. A. Salyers, A. Gupta, and Y. Wang, Human intestinal bacteria as reservoirs for antibiotic resistance genes, TRENDS in Microbiology, 2004,12(9), 0-416. (DOI: 10.1016/j.tim.2004.07.004)
9. M. J. Feio, I. Sousa, M. Ferreira, L. Cunha-Silva, R. G. Saraiva, C. Queiros, J. G. Alexandre, V. Claro, A. Mendes, R. Ortiz, S. Lopes, A. L. Amaral, J. Lino, P. Fernandes, A. J. Silva, L. Moutinho, B. De Castro, E. Pereira, L. Perello, and P. Gameiro, Fluoroquinolone-metal complexes: a route to counteract bacterial resistance? Journal of Inorganic Biochemistry, 2014, 138, 129-143. (DOI: 10.1016/j.jinorgbio.2014.05.007)
10. P. Cervini, B. Ambrozini, L. Carlos, M. M. Ana, and P. Garcia, Thermal behavior and decomposition of oxytetracycline hydrochloride, J Therm Anal Calorim, 2015, 121(1), 347-352. (DOI: 10.1007/s10973-015-4447-x)
11. V. L. Pham, D. Kim, and S. Ko, Oxidative degradation of the antibiotic oxytetracycline by Cu@Fe_3O_4 core-shell nanoparticles, Science of the Total Environment, 2018, 631-632, 608-618. (DOI: 10.1016/j.scitotenv.2018.03.067)

12. S. Orellana, C. Soto, and M. I. Toral, UV–vis, IR and 1H NMR spectroscopic studies and characterization of ionic-pair crystal violet–Oxytetracycline, Spectrochimica Acta Part A: Molecular and Biomolecular Spectroscopy,2010, 75(1), 437-443. (DOI:10.1016/j.saa.2009.11.002)

13. W. Qi, J. Long, C. Feng, Y. Feng, and D. Cheng, Fe^{3+} enhanced degradation of oxytetracycline in water by pseudomonas, Water Research, 2019, 160, 361. (DOI: 10.1016/j.watres.2019.05.058)

14. F. Yin, H. Dong, W. Zhang, Z. Zhu, and B. Shang, Antibiotic degradation and microbial community structures during acidification and methanogenesis of swine manure containing chlortetracycline or Oxytetracycline, Bioresource Technology, 2017, 250, 247. (DOI: 10.1016/j.biortech.2017.11.015)

15. O. A. Arikan, L. J. Sikora, W. Mulbry, S. U. Khan, C. Rice, and G. D. Foster, The fate and effect of oxytetracycline during the anaerobic digestion of manure from therapeutically treated calves, Process Biochemistry, 2006, 41(7), 1637-1643. (DOI:10.1016/j.procbio.2006.03.010)

16. A. Zianna, G. D. Geromichalos, and A. G. Hatzidimitriou, Palladium(II) complexes with salicylaldehyde ligands: Synthesis, characterization, structure, in vitro and in silico study of the interaction with calf-thymus DNA and albumins, Journal of Inorganic Biochemistry, 2019, 194, 85. (DOI:10.1016/j.jinorgbio.2019.02.013)

17. H. Kargar, V. Torabi, A. Akbari, and R. Behjatmanesh-ardakani, Pd(II) and Ni(II) complexes containing an asymmetric Schiff base ligand: Synthesis, x-ray crystal structure, spectroscopic investigations, and computational studies, Journal of Molecular Structure, 2020, 1205, 127642. (DOI:10.1016/j.molstruc.2019.127642)

18. R. K. Sharma, and C. Sharma, Zirconium(IV)-modified silica gel: Preparation, characterization and catalytic activity in the synthesis of some biologically important molecules, CATCOM, 2011,12(5), 327-331.(DOI: 10.1016/j.catcom.2010.10.011)

19. L. M. Mirica, and J. R. Khusnutdinova, Structure and electronic properties of Pd(III) complexes, Coordination Chemistry Reviews, 2013,257(2), 299-314. (DOI: 10.1016/j.ccr.2012.04.030)

20. V. Nagalakshmi, M. Sathya, M. Premkumar, D. Kaleeswaran, G. Venkatachalam, and K. Balasubramani, Palladium(II) Complexes comprising Naphthylamine and Biphenylamine based Schiff base Ligands: Synthesis, Structure and Catalytic activity in Suzuki coupling reactions, Journal of Organometallic Chemistry, 2020, 121220. (DOI: 10.1016/j.jorganchem.2020.121220)

21. S. Rubino, R. Busà, A. Attanzio, R. Alduina, V. Di. Stefano, M. A. Girasolo, S. Orecchio, and L. Tesoriere, Synthesis, properties, antitumor and antibacterial activity of new Pt(II) and Pd(II) complexes with 2,2'-dithiobis(benzothiazole) ligand, Bioorganic & Medicinal Chemistry, 2017, 25, 2378. (DOI: 10.1016/j.bmc.2017.02.067)

22. C. D. Miranda, and R. Zemelman, Bacterial resistance to oxytetracycline in Chilean salmon farming, Aquaculture, 2002, 212(1-4), 31-47. (DOI: 10.1016/S0044-8486(02)00124-2)

23. O. B. Samuelsen, V. Torsvik, and A. Ervik, Long-range changes in oxytetracycline concentration and bacterial resistance towards oxytetracycline in a fish farm sediment after medication, The Science of the Total Environment, 1992, 114, 25-36. (DOI: 10.1016/0048-9697(92)90411-K)

24. M. M. El-ajaily, H. A. Abdullah, A. Al-janga, E. E. Saad, and A. A. Maihub, Zr(IV), La(III), and Ce(IV) Chelates with 2-[(4-[(Z)-1-(2-Hydroxyphenyl)ethylidene]aminobutyl)-ethanimidoyl] phenol: Synthesis, Spectroscopic Characterization, and Antimicrobial Studies. Advances in Chemistry, 2015, 1–16.(DOI:10.1155/2015/987420)

25. W. Guerra, E. de.A. Azevedo, A. R. de. S. Monteiro, M. Bucciarelli-Rodriguez, E. Chartone-Souza, A. M. A. Nascimento, A. P. S. Fontes, L. Le Moyec, and E. C. Pereira-Maia, Synthesis, characterization, and antibacterial activity of three Palladium (II) complexes of tetracyclines, Journal of Inorganic Biochemistry, 2005, 99, 2348–2354. (DOI: 10.1016/j.jinorgbio.2005.09.001)

26. A. T. Fiori-duarte, F. R. G. Bergamini, R. Enoque, F. De. Paiva, C. M. Manzano, W. R. Lustri, and P. P. Corbi, A new palladium(II) complex with ibuprofen: Spectroscopic characterization, DFT studies, antibacterial activities and interaction with biomolecules, Journal of Molecular Structure, 2019, 1186, 144. (DOI: 10.1016/j.molstruc.2019.03.020)

27. P. Kavitha, and K. L. Reddy, Pd(II) complexes bearing chromone based Schiff bases: Synthesis, characterization and biological activity studies, ARABIAN JOURNAL OF CHEMISTRY, 2016,9, 640. (DOI: 10.1016/j.arabjc.2013.06.018)

28. G. D. Bajju, G. Devi, S. Katoch, M. Bhagat, S. Kundan, and S. K. Anand, Synthesis, Spectroscopic, and Biological Studies on New Zirconium(IV) Porphyrins with Axial Ligand, Bioinorganic Chemistry, and Applications, 2013, 15. (DOI:10.1155/2013/903616)

29. K. A. Abu-safieh, A.S. Abu-surrah, H. D. Tabba, H. A. Almasri, R. M. Bawadi, F. M. Boudjelal, and L. H. Tahtamouni, Novel Palladium(II) and Platinum(II) Complexes with a Fluoropiperazinyl Based Ligand Exhibiting High Cytotoxicity and Anticancer Activity In Vitro, Journal of Chemistry, 2016,7. (DOI: 10.1155/2016/7508724)

30. S. Chandra, M. Tyagi, and S. Agrawal, Spectral and antimicrobial studies on tetraaza macrocyclic complexes of Pd^{II}, Pt^{II}, Rh^{III}, and Ir^{III} metal ions, Journal of Saudi Chemical Society,2011**,** 15(1), 49-54. (DOI: 10.1016/j.jscs.2010.09.005)

31. Z. Tan, F. Tan, L. Zhao, and J. Li, The Synthesis, Characterization, and Application of Ciprofloxacin Complexes and Its Coordination with Copper, Manganese and Zirconium Ions, Journal of Crystallization Process and Technology, 2012, 2, 55-63. (DOI: 10.4236/jcpt.2012.22008)

32. Z. Ghadamyari, A. Shiri, A.Khojastehnezhad, and S. M. Seyedi, Zirconium (IV) porphyrin graphene oxide: a new and efficient catalyst for the synthesis of 3, 4-dihydro pyrimidine- 2(1H)-ones, Appl Organometal Chem., 2019,1. (DOI: 10.1002/aoc.5091)

33. M. Gupta, S. Sihag, A. K. Varshney, and S. Varshney, Synthesis, Structural, and Antimicrobial Studies of Some New Coordination Compounds of Palladium(II) with Azomethines Derived from Amino Acids,J ournal of Chemistry, 2013, 8. (DOI: 10.1155/2013/745101)

34. A. Chaudhary, and A. Singh, Synthesis, Characterization, and Evaluation of Antimicrobial and Antifertility Efficacy of Heterobimetallic Complexes of Copper (II), Journal of Chemistry, 2017, 9. (DOI: 10.1155/2017/5936465)

35. S. I. Islam, S. B. Das, S. Chakrabarty, S. Hazra, A. Pandey, and A. Patra, Synthesis, Characterization, and Biological Activity of Nickel (II) and Palladium (II) Complex with Pyrrolidine Dithiocarbamate (PDTC), Advances in Chemistry, 2016, 6. (DOI: 10.1155/2016/4676524)

36. D. Kumar, S. Chadda, J. Sharma, and P. Surain, Syntheses, Spectral Characterization, and Antimicrobial Studies on the Coordination Compounds of Metal Ions with Schiff Base Containing Both Aliphatic and Aromatic Hydrazide Moieties,Bioinorganic Chemistry and Applications, 2013, 10. (DOI:10.1155/2013/981764)

37. F. A. El-Saied, M .M. E. Shakdofa, A. S.El Tabl, M. M. Abd-Elzaher, and N. Morsy, Coordination versatility of N_2O_4 polydentate hydrazonic ligand in Zn(II), Cu(II), Ni(II), Co(II), Mn(II) and Pd(II) complexes and antimicrobial evaluation, Journal of Basic and Applied Sciences, 2017, 6, 310. (DOI:10.1016/j.bjbas.2017.09.005)

38. A. K. Singh, and U. T. Nakate, Microwave Synthesis, Characterization, and Photoluminescence Properties of Nanocrystalline Zirconia, The scientific world journal, 2014, 7. (DOI: 10.1155/2014/349457)

39. G .D. Bajju, G. Devi, S. Katoch, M. Bhagat, Deepmala, Ashu, S. Kundan, and S. K. Anand, Synthesis, spectroscopic, and biological studies on new Zirconium (IV) porphyrins with an axial ligand. Bioinorganic Chemistry and Applications, 2013, 15. (DOI: 10.1155/2013/903616)

40. N. Nakata, K. Nakamura, S. Nagaoka, and A. Ishii, Carbazolyl-Substituted [OSSO]-Type Zirconium(IV) Complex as a Precatalyst for the Oligomerization and Polymerization of α-Olefins, Catalysts, 2019, 9(6), 528. (DOI: 10.3390/catal9060528)

41. M. Mandal, M. List, I. Teasdale, D. Chakraborty, and U. Monkowius, Palladium complexes containing imino phenoxide ligands: synthesis, luminescence, and their use as catalysts for the ring-opening polymerization of rac-lactide, Monatsh Chem, 2017, 1. (DOI: 10.1007/s00706-017-2119-1)

42. H. V. Huynh, D. Le. Van, F. E. Hahn, and T. S. A. Hor, Synthesis and structural characterization of mixed carbene-carboxylate complexes of palladium(II), Journal of Organometallic Chemistry, 2004, 689(10), 1766-1770. (DOI: 10.1016/j.jorganchem.2004.02.033)

43. D. P. Steinhuebel, P. Fuhrmann, and S. J. Lippard, Synthesis, characterization, and reactivity of organometallic Zr(IV) carboxylate complexes, Inorganica Chimica Acta, 1998, 270, 527. (DOI: 10.1016/S0020-1693(97)06117-3)

44. N. Smrečki, J. Jaźwiński, and Z. Popović, Preparation and NMR spectroscopic study of palladium(II) complexes with N-arylalkyliminodiacetamide derivatives, Journal of Molecular Structure, 2016, 1122, 192. (DOI: 10.1016/j.molstruc.2016.05.084)

45. H. L. Singh, and J. Singh, Synthesis of New Zirconium(IV) Complexes with Amino Acid Schiff Bases: Spectral, Molecular Modeling, and Fluorescence Studies, International Journal of Inorganic Chemistry, 2013, 1-10. (DOI: 10.1155/2013/847071)

46. W. Hernandez, J. Paz, F. Carrasco, A. Vaisberg, E. Spodine, J. Manzur, and L. Beyer, Bioinorganic Chemistry and Applications, 2013,12. (DOI: 10.1155/2013/524701)

47. W. H. El-Shwiniy, W. S. Shehab, S. F. Mohamed, and H. G. Ibrahium, Applied Organometallic Chemistry, 2018, 32, 1. (DOI: 10.1002/aoc.4503)

48. K. I. Khallow, and A. Y. R. Al-Assaf, E-Journal of Chemistry, 2011, 8, 576.

49. I. M. I. Moustafa, and M. H.Abdellattif, Mod Chem Appl, 2017,5. (DOI: 10.4172/2329-6798.1000202)

50. S. Tetteh, D. K. Dodoo, R. Appiah-opong, and I. Tuffour, Journal of Inorganic Chemistry, 2014, 7. (DOI: 10.1155/2014/586131)

51. P.A.Ajibade, and O. G. Idemudia, Bioinorganic Chemistry and Applications, 2013, 8. (DOI: 10.1155/2013/54954)

52. A. J. Abdul-Ghani, and A. M. N. Khaleel, Bioinorganic Chemistry and Applications, 2009,12. (DOI:10.1155/2009/413175)

53. S. A. Shaker, Synthesis and Study of Mixed Ligand-Metal Complexes of 1, 3, 7-Trimethylxanthine and 1, 3-Dimethyl-7H-purine-2, 6-dione with Some Other Ligands E-Journal of Chemistry, 2010, 8(1), 153-158

54. A. A. Abdel Aziz, A. N. M. Salem, M. A. Sayed, and M. M. Aboaly, Synthesis, structural characterization, thermal studies, catalytic efficiency and antimicrobial activity of some M(II) complexes with ONO tridentate Schiff base N-salicylidene-o-aminophenol (saphH2), Journal of Molecular Structure, 2012, 1010, 130-138. (DOI:10.1016/j.molstruc.2011.11.043)

55. M. Gaber, H. El-ghamry, F. Atlam, and S. Fathalla, Synthesis, spectral and theoretical studies of Ni(II), Pd(II) and Pt(II) complexes of 5-mercapto-1,2,4-triazole-3-imine-20–hydroxynaphyhaline, SPECTROCHIMICA ACTA PART A: MOLECULAR AND BIOMOLECULAR SPECTROSCOPY, 2015, 137, 919-929. (DOI:10.1016/j.saa.2014.09.015)

56. M. Montazerozohori, S. Zahedi, A. Naghiha, and M. M. Zohour, Synthesis, characterization and thermal behavior of antibacterial and antifungal active zinc complexes of bis (3(4-dimethylaminophenyl)-allylidene-1,2-diaminoethane, Materials Science & Engineering, 2014, 35, 195-204. (DOI:10.1016/j.msec.2013.10.030)

57. S. M. Prabhu and S. Meenakshi, Novel one-pot synthesis of dicarboxylic acids mediated alginate zirconium biopolymeric complex for defluoridation of water, Carbohydrate Polymers, 2015, 120, 60-68. (DOI: 10.1016/j.carbpol.2014.11.058)

58. S. Sobhani, and F. Zarifi, Pd-isatin Schiff base complex immobilized on γ-Fe2O3 as a magnetically recyclable catalyst for the Heck and Suzuki cross-coupling reactions, Chinese Journal of Catalysis, 2015, 36(4), 555-563. (DOI: 10.1016/S1872-2067(14)60291-6)

59. A. Benyei, and I. Sovago, Thermodynamic, kinetic and structural studies on the mixed ligand complexes of palladium(II) with tridentate and monodentate ligands, Journal of Inorganic Biochemistry, 2003, 94(3), 291-299. (DOI: 10.1016/S0162-0134(03)00009-6)

60. L. H. Abdel-rahman, M. Shaker, S. Adam, N. Al-zaqri, M. R. Shehata, H. E. Ahmed, and S. K. Mohamed, Synthesis, characterization, biological and docking studies of ZrO (II), VO (II) and Zn (II) complexes of a halogenated tetra-dentate Schiff base. Arabian Journal of Chemistry, 2022, 15(5), 103737. (DOI: 10.1016/j.arabjc.2022.103737)

61. D. A. Milenkovi´c, D. S. Dimi´c, E. H. Avdovi´c, and Z. S. Markovi´c, (2020). Several coumarin derivatives and their Pd(II) complexes as potential inhibitors of the main protease of SARS-CoV-2, an in silico approach†. RSC Adv., 2020,10(58), 35099–35108. (DOI: 10.1039/d0ra07062a)

62. A. Zianna, G. D. Geromichalos, A. Pekou, G. Hatzidimitriou, E. Coutouli-argyropoulou, M. Lalia-Kantouri, A. A. Pantazaki, and G. Psomas, A palladium(II) complex with the Schiff base 4-chloro-2-(N-ethyliminomethyl)-phenol: Synthesis, structural characterization, and *in vitro* and *in silico* biological activity studies,Journal of Inorganic Biochemistry, 2019, 199(Ii), 110792. (DOI:10.1016/j.jinorgbio.2019.110792)

63. S. Guti, J. Espino, F. Luna-giles, A. B. Rodr, J. A. Pariente, and E. Viñuelas-zah, Synthesis, Characterization and Antiproliferative Evaluation of Pt (II) and Pd (II) Complexes with a Thiazine-Pyridine Derivative Ligand †. Pharmaceuticals, 2021, 14, 395. (DOI: 10.3390/ph14050395)

64. A. Kerflani, K. Si, A. Rabahi, A., Bouchoucha, and S. Zaater, Inorganica Chimica Acta Novel palladium (II) complexes with iminocoumarin ligands: Synthesis, characterisation, electrochemical behaviour, DFT calculations and biological activities, ADMET study and molecular docking. Inorganica Chimica Acta, 2021, 529, 120659. (DOI: 10.1016/j.ica.2021.120659)

65. D. Kumar, and A. Kumar, Physicochemical, Spectral, and Biological Studies of Mn(II), Cu(II), Cd(II), Zr(OH)2(IV), and UO2(VI) Compounds with Ligand Containing Thiazolidin-4-one Moiety, Journal of Chemistry, 2014, 9. (DOI: 10.1155/2014/286136)

66. H. G. Aslan, S. Özcan, and N. Karacan, Synthesis, characterization and antimicrobial activity of salicylaldehyde benzene sulfonyl hydrazone (Hsalbsmh) and its Nickel(II), Palladium(II), Platinum(II), Copper(II), Cobalt(II) complexes, INOCHE, 2011, 14(9), 1550-1553. (DOI: 10.1016/j.inoche.2011.05.024)

67. S. Andotra, S., Kumar, M. Kour, N. Kalgotra, and S. K. Pandey, Spectroscopic, thermal, quantum chemical calculations and in vitro biological studies of titanium/zirconium(IV) complexes of mono-and disubstituted aryldithiocarbonates, Journal of Molecular Structure, 2018, 1155, 215. (DOI:10.1016/j.molstruc.2017.10.082)

68. D. L. Stojković, V. V. Jevtić, N. Vuković, M. Vukić, P. Čanović, M. M. Zarić, M. M., Mišić, D. M., Radovanović, D. Baskić, and S. R.Trifunović,Synthesis, characterization, antimicrobial and antitumor reactivity of new palladium(II) complexes with methionine and tryptophane coumarine derivatives, Journal of Molecular Structure, 2018, 1157, 425. (DOI: 10.1016/j.molstruc.2017.12.095)

69. W. H. El-shwiniy, and W. A. Zordok, Synthesis, spectral, DFT modeling, cytotoxicity and microbial studies of novel Zr(IV), Ce(IV) and U(VI) piroxicam complexes, Spectrochimica Acta Part A: Molecular and Biomolecular Spectroscopy, 2018,199, 290. (DOI: 10.1016/j.saa.2018.03.074)